RESEARCH ARTICLE

Eliminating yellow fever epidemics in Africa: Vaccine demand forecast and impact modelling

Kévin Jean [1,2,3]*, **Arran Hamlet** [3], **Justus Benzler** [4,5], **Laurence Cibrelus** [4], **Katy A. M. Gaythorpe** [3], **Amadou Sall** [6], **Neil M. Ferguson** [3], **Tini Garske** [3]

1 Laboratoire MESuRS, Conservatoire National des Arts et Métiers, Paris, France, **2** Unité PACRI, Institut Pasteur, Conservatoire National des Arts et Métiers, Paris, France, **3** MRC Centre for Global Infectious Disease Analysis, Department of Infectious Disease Epidemiology, Imperial College, St Mary's Campus, Norfolk Place London, United Kingdom, **4** Infectious Hazard Management, World Health Organization, Geneva, Switzerland, **5** Robert Koch-Institut, Nordufer, Berlin, Germany, **6** Arbovirus and viral haemorrhagic fever unit, Institut Pasteur de Dakar, Dakar, Senegal

* kevin.jean@lecnam.net

Abstract

Background

To counter the increasing global risk of Yellow fever (YF), the World Health Organisation initiated the Eliminate Yellow fever Epidemics (EYE) strategy. Estimating YF burden, as well as vaccine impact, while accounting for the features of urban YF transmission such as indirect benefits of vaccination, is key to informing this strategy.

Methods and findings

We developed two model variants to estimate YF burden in sub-Saharan Africa, assuming all infections stem from either the sylvatic or the urban cycle of the disease. Both relied on an ecological niche model fitted to the local presence of any YF reported event in 34 African countries. We calibrated under-reporting using independent estimates of transmission intensity provided by 12 serological surveys performed in 11 countries. We calculated local numbers of YF infections, deaths and disability-adjusted life years (DALYs) lost based on estimated transmission intensity while accounting for time-varying vaccination coverage. We estimated vaccine demand and impact of future preventive mass vaccination campaigns (PMVCs) according to various vaccination scenarios.

Vaccination activities conducted in Africa between 2005 and 2017 were estimated to prevent from 3.3 (95% CI 1.2–7.7) to 6.1 (95% CI 2.4–13.2) millions of deaths over the lifetime of vaccinees, representing extreme scenarios of none or maximal herd effects, respectively. By prioritizing provinces based on the risk of urban YF transmission in future PMVCs, an average of 37.7 million annual doses for PMVCs over eight years would avert an estimated 9,900,000 (95% CI 7,000,000–13,400,000) infections and 480,000 (180,000–1,140,000) deaths over the lifetime of vaccinees, corresponding to 1.7 (0.7–4.1) deaths averted per 1,000 vaccine doses.

Conclusions

By estimating YF burden and vaccine impact over a range of spatial and temporal scales, while accounting for the specificity of urban transmission, our model can be used to inform the current EYE strategy.

Author summary

As large-scale vaccination campaigns are begun or continued with the aim to eliminate yellow fever (YF) epidemics in several countries, estimating disease burden and vaccine impact is timely. We developed two model variants to estimate YF burden in sub-Saharan Africa, each either representing the sylvatic or urban cycle of the disease. Both relied on an ecological niche model fitted to known records of YF in 34 African countries and calibrated using serological survey data. Local numbers of YF infections and deaths were derived while accounting for time-varying vaccination coverage. We estimated vaccine demand and the impact of future preventive mass vaccination campaigns according to various vaccination scenarios. By providing burden and vaccine impact estimates over a range of spatial and temporal scales, and accounting for the specificity of urban transmission, our model can be used to inform the current international strategy to counter the increasing global risk of yellow fever.

Introduction

Recent outbreaks in Angola, Nigeria and Brazil have shown that yellow fever (YF) remains a significant public health threat [1,2]. The epidemics of Zika and chikungunya in Latin America have also highlighted the risks of international spread of arboviruses. The spread of YF to Asia, where the virus has not yet been detected despite the presence of competent vectors, could have a major negative public health impact [3,4]. In response, in 2016, the World Health Organisation (WHO) adopted a strategy to Eliminate Yellow fever Epidemics (EYE) by 2026. This strategy aims to prevent sporadic cases sparking urban outbreaks, thus minimizing the risk of international spread [5]. The EYE strategy largely relies on, but is not limited to, scale-up of vaccination.

Vaccination activities considered in the EYE strategy consist of routine immunization of infants, preventive mass vaccination campaigns (PMVCs) that target all or most age groups, preventive catch-up campaigns targeting specific cohorts or unvaccinated sub-populations, and reactive campaigns in outbreak situations. Local assessment of YF transmission intensity is key for the prioritization of each of these vaccination activities; particularly since the supply of vaccine is limited as seen during the 2016 Angola outbreak [6,7]. Vaccine demand forecasts are critical to shape vaccine production and ensure optimal vaccine allocation.

Previous mathematical models have assessed geographical heterogeneity in YF risk [8–10]. However, modelling YF is challenging because of the co-existence of different transmission cycles [11]. In the sylvatic cycle, tree-dwelling mosquitoes transmit the virus within the wildlife reservoir (non-human primates) and spill-over infection may occur for humans living or working in jungle habitats. In the urban cycle, the domestic mosquito *Aedes aegypti* transmits the virus between humans. Population ('herd') immunity (whether via natural infection or vaccination) will be expected to modify transmission intensity within the urban cycle, but not in the sylvatic cycle where transmission intensity is driven by non-human primates and their

interactions with human populations. Recently, two models quantifying the incidence of the disease in Africa or worldwide have been used to derive estimates for vaccination impact [9,10]. Both assumed a constant force of infection over time. A static force of infection, unaffected by susceptible fraction in the population reflects the sylvatic rather than the urban transmission cycle of the disease. As a corollary, these models disregarded possible herd effects that may arise in urban context due to changing population-level immunity.

Recent evidence suggested the sylvatic YF transmission cycle to be predominant in the Brazilian epidemiological context [12]. However, there is a consensus that both urban and sylvatic transmission cycles play significant roles in the global burden of YF in Africa, though the relative contribution of each is unknown [5,13]. In the absence of estimates of the relative contribution of zoonotic versus human-to-human transmission, one approach could consist in exploring both extreme scenarios of 100% of sylvatic versus urban transmission. Such an approach would allow to compare burden estimates and vaccine impact while disregarding or maximizing, respectively, the effect of herd immunity.

Accelerated urbanization and increasing human population mobility might increase the contribution of the urban transmission cycle to the global YF burden. Urban cases have the potential to trigger explosive outbreaks that can place a substantial burden on health systems, as well as causing significant social and economic impacts. Both the large number of cases arising in urban outbreaks, and the higher connectivity of affected populations compared to the, typically, much more remote settings in which sylvatic transmission occurs, make international spread more likely. Thus, accounting for specific features of urban transmission will be useful to assess the risk of urban outbreaks and refine the estimates of vaccine impact.

In this paper, we have extended a previously developed model [9] to account for specific features of inter-human transmission. We then compare this model to the previous version (which focussed on sylvatic transmission) and update previous estimates of YF burden and vaccine impact, accounting for indirect effects. Lastly, based on local estimates of the potential for inter-human urban transmission, we propose different scenarios of PMVCs that could be considered for the EYE strategy, evaluating vaccine demand and impact in terms of infections and mortality averted.

Methods

The Yellow Fever burden model [9] was developed to estimate YF disease burden and vaccine impact across 34 African countries at high or moderate risk for YF [5]. The original model was developed assuming that the locally-fitted force of infection (the annual probability of infection for a susceptible individual), λ, was constant in time. Here, we updated the previous constant version of the model by integrating novel serological data updating demographic data as well as recent vaccination activities and records of the disease. Moreover, we present a new, alternative, variant of the model parametrised by the locally-fitted basic reproduction number R_0, which allows the resulting force of infection to vary dynamically as population-level immunity changes over time.

Model overview

A complete description of the model is available in S1 Appendix. Briefly, both model variants include a generalized linear model (GLM) fitted to the presence or absence of any reported YF event between 1984 and 2013 at the first sub-national administrative level (province) (S1 Table), using various environmental and demographic covariates together with a country-based proxy for surveillance quality. We defined a reported YF event as either outbreak reports

published by WHO or laboratory-confirmed cases reported in a YF surveillance database managed by WHO-AFRO, to which 21 countries contribute.

The GLM provides estimates of the probability of any YF report across the endemic zone over the 30-year period considered. In a second step, we describe this probability of a report as dependent on the number of infections and on the unknown rate of under-reporting (which was assumed to vary between but not within countries). This latter parameter was calibrated to independent estimates of transmission intensity, obtained by fitting 12 serological surveys performed in 11 African countries.

The two model versions differ in the way they fit serological data. In the static version of the model (FOI model) a constant, age-independent force of infection (FOI) λ is fitted to each serological survey. Alternatively, in the dynamical version of the model (R_0 model), a basic reproduction number R_0 is fitted, based on the classical SIR model framework under the assumption of endemic equilibrium transmission [14].

The GLM quantifies geographic variation of the relative risk of YF report across the continent while each serological survey yields an estimate of the absolute transmission intensity in its specific location. For each of the 31 survey locations we can therefore estimate the local level of under-ascertainment by tying GLM predictions to estimated values of λ or R_0 whilst accounting for time-dependent vaccination coverage [15]. This level of under-ascertainment was then extrapolated across the endemic zone and the absolute transmission intensity was then inferred by combining it with the probability of YF report.

By extrapolating this estimated level of under-ascertainment, we may infer the absolute transmission intensity across the continent from the GLM predictions.

The main difference in the dynamics of the FOI and R_0 models lies in the way they respond to vaccination. In the FOI model, the susceptible population is reduced by vaccination but the per-capita risk of infection of remaining susceptible individuals remains unchanged, always resulting in a non-zero number of new infections with imperfect vaccination coverage. In contrast, the R_0 model responds non-linearly to vaccination coverage: if, for a specific year, vaccination activities happen to increase the immunized proportion of the population above the herd immunity threshold, $1 - 1/R_0$ (the formula defining the critical vaccination coverage), then we assumed that no new infection will be expected in that year. In that case, the unvaccinated proportion of the population is indirectly but fully protected by herd immunity. Note that when there is no history of vaccination, the R_0 model reproduces the FOI model.

Model fitting and burden estimates

The model is fitted in a Bayesian framework using Markov chain Monte Carlo simulations. We assumed a prior distribution for vaccine efficacy centred at 97.5% (95% confidence intervals: 82.9% to 99.7%) [16], with no waning of immunity [17]. The models were fitted based on the best yearly estimates of vaccination coverage [15]. Posterior samples of parameters were used to compute medians and 95% credibility intervals (CI) of model parameters and burden estimates.

Both models predict spatiotemporally varying incidence of YF infections. We assumed that 12% (95% CI: 5% to 26%) of all infections develop severe disease and a case fatality ratio among severe cases of 47% (95% CI: 31% to 62%) [18] to translate infection incidence estimates into numbers of severe cases, deaths and disability-adjusted life years (DALYs) lost (S1 Appendix).

We further calculated vaccine impact of past vaccination activities by estimating the burden expected had these activities not taken place (S1 Appendix). We defined the lifetime impact of vaccination as the cumulative burden difference over the 2000–2100 time period between the

baseline scenario, ie the burden calculated using the best estimates of vaccination coverage, and a counterfactual scenario of no vaccination. For each scenario, we summed the burden across each year between 2000–2100 and across all ages, before calculating the difference between the no-vaccination and the baseline scenario. Considering such a time horizon ensures we capture vaccine impact over most of the lifetime of people vaccinated and those benefitting from the resulting herd immunity.

Model validation

We conducted an out-of-sample validation process using the data of three recent serological surveys from the Democratic Republic of Congo, South Sudan and Chad in 2015. To our knowledge, these serological surveys were the latest available in the endemic region at the time we conducted this research.

Validation was conducted by comparing: i) transmission parameters estimated by fitting the age-seroprevalence profiles from those surveys to those predicted for the corresponding provinces in the YF burden model, ii) age-seroprevalence profiles directly observed in the surveys to those predicted by the YF burden model (S2 Appendix).

Estimating vaccine demands and impact of large-scale vaccination campaigns

Lastly, we estimated the number of doses needed for, and the impact of, possible future PMVCs. As the EYE strategy aims to prevent outbreaks and international spread, we focused on the R_0 model which better captures urban transmission. We estimated the effective reproduction number R_{eff} describing the transmission potential in a partially immune population across the endemic region as $R_{eff} = R_0(1-vc)$, where vc is the 2018 vaccine-acquired population-level immunity. Based on different R_{eff} threshold values, four vaccination strategies were simulated in which provinces were eligible for PMVCs: i) $R_{eff} \geq 1.25$ (strategy A), ii) $R_{eff} \geq 1.01$ (strategy B), iii) $R_{eff} \geq 1.00$ (strategy C), and iv) $R_{eff} \geq 0.85$ (strategy D). These strategies thus rank from a parsimonious strategy focussed on high-risk areas (strategy A) to an ambitious large-scale strategy provinces with a broader range of transmission risk (strategy D). We compared the strategies with each other under the optimistic assumptions of: i) maximized herd effects as per the use of the R_0 model variant, and ii) an optimal sequence of PMVC implementation. For each strategy, the total target population was estimated. The corresponding number of vaccine doses was attributed to provinces based on a ranking of R_{eff} values, so provinces with the highest R_{eff} values were vaccinated first (2018) and those with the lowest R_{eff} value were vaccinated last (2026). Vaccination campaigns were assumed to reach 90% of the population, regardless of age or previous vaccination status. For each strategy, the lifetime impact of PMVCs was estimated through comparison with a baseline scenario assuming no further reactive or preventive vaccination campaigns, but an annual 1%-increase in the coverage of routine immunization (capped at 90%) from their 2015 levels in countries where routine immunization already includes YF vaccine.

Results

Based on existing surveillance data and publicly-available reports, YF had been reported at least once over the 1984–2013 period in 160 of 479 provinces (Fig 1A). Relying on various environmental and demographic covariates, the GLM reproduced the presence/absence of YF well with an area under the ROC curve >0.9 for both model variants (Table 1 and S1 Fig).

We used the results of serological surveys conducted between 1985 and 2014 in 31 different locations (Fig 1B) to calibrate the models. Seroprevalence among unvaccinated participants
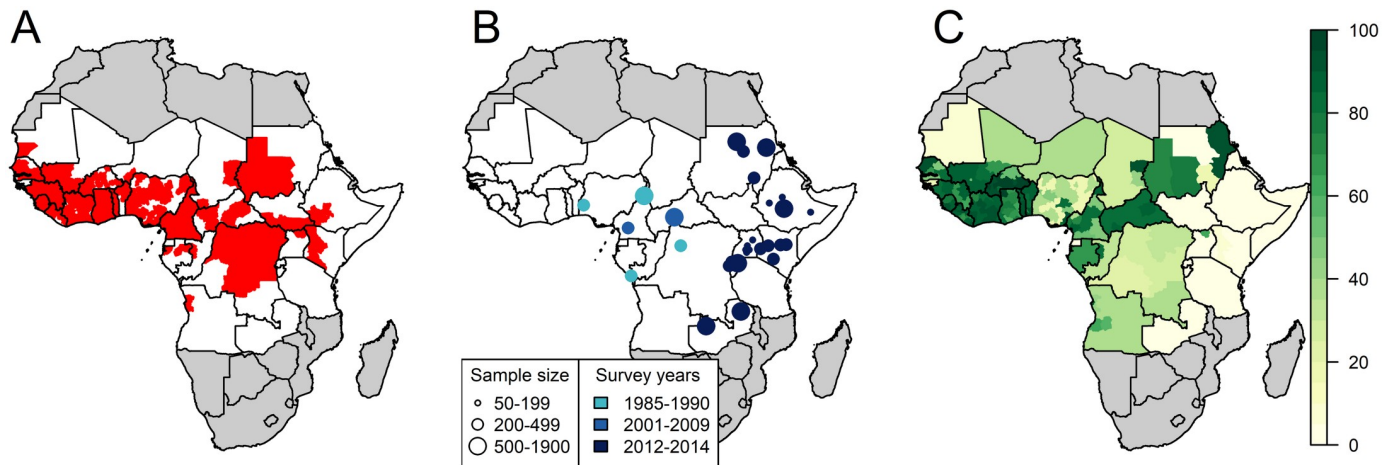
Fig 1. Input data of the model. A: presence (red) or absence (white) of any yellow fever report between 1984 and 2013. B: Location, sample size and study years 12 serological surveys covering 31 provinces. C: estimated population-level vaccination coverage for 2017. Maps were produced from GADM version 2.0.

https://doi.org/10.1371/journal.pntd.0008304.g001

ranged from 0.0% in northern Kenya in 2013 (95% CI: 0.0–0.9%) to 20.1% (15.0–26.5%) in South-West Nigeria in 1990. Population-level vaccination coverage estimates for 2017 ranged from 0.0% in various regions of Eastern Africa to 96.6% in several provinces of Burkina Faso (Fig 1C).

Table 1. Parameter estimates and outcomes for both model variants.

	FOI model, median estimate (95% Credibility Interval)	R$_0$ model, median estimate (95% Credibility Interval)
Model parameters		
GLM Area under the Curve	0.916 (0.909–0.921)	0.916 (0.908–0.921)
Minimum per-infection probability of detection	3.6e-7 (2.1e-8–2.9e-6), Guinea-Bissau	6.2e-7 (4.5e-8–3.6e-6), Guinea-Bissau
Maximum per-infection probability of detection	1.9e-5 (9.0e-6–3.8e-5), Central African Republic	3.0e-5 (1.8e-5–5.1e-5), Central African Republic
Vaccine efficacy	0.952 (0.749–0.993)	0.942 (0.671–0.993)
Burden estimates		
1995 number of deaths	110,000 (40,000–280,000)	120,000 (50,000–320,000)
2005 number of deaths	130,000 (50,000–320,000)	60,000 (20,000–210,000)
2017 number of deaths	110,000 (40,000–270,000)	30,000 (4,000–120,000)
2017 number of severe cases	240,000 (90,000–620,000)	70,000 (9,000–270,000)
2017 total number of infections	2,190,000 (1,310,000–3,710,000)	670,000 (100,000–1,790,000)
2017 total number of DALYs lost	5,400,000 (1,900,000–13,600,000)	1,700,000 (240,000–7,000,000)
Lifetime vaccine impact estimates of 2005–2017 PMVCs*		
Deaths prevented	3,300,000 (1,200,000–7,700,000)	6,100,000 (2,400,000–13,200,000)
DALY prevented	145,800,000 (53,700,000–345,700,000)	327,900,000 (133,000,000–699,300,000)

DALYs: disability-adjusted life years; PMVCs: Preventive mass vaccination campaigns.

*Lifetime vaccine impact is defined as the cumulative difference over the 2000–2100 time period in baseline burden estimates and those estimated had the 2005–2017 PMVCs not taken place. The 2000–2100 time horizon ensures to capture vaccine impact over most of the lifetime of people vaccinated and those benefitting from the resulting herd immunity.
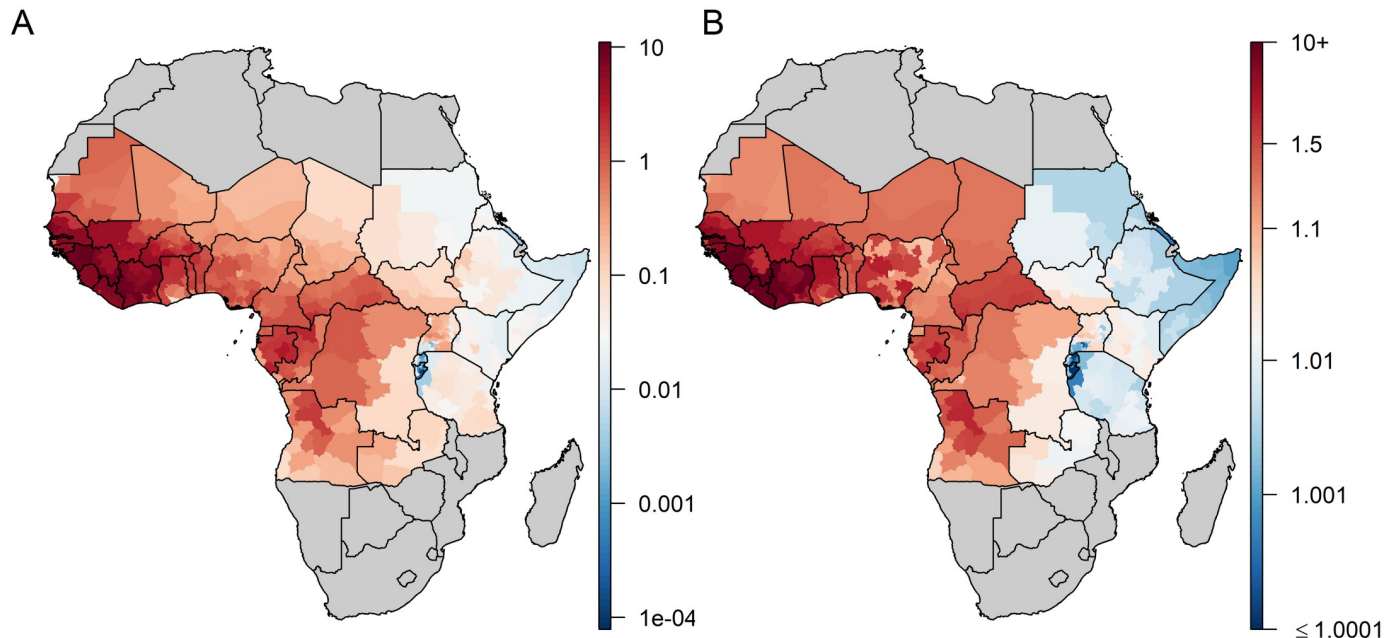
https://doi.org/10.1371/journal.pntd.0008304.t001

Fig 2. Estimates of transmission intensity in the FOI (A) versus the R₀ (B) model variants. A: median estimates of the force of infection (FOI), in %; B: median estimates of R_0. Maps were produced from GADM version 2.0.

We estimated per-infection probabilities of detection by combining GLM predictions and results of serological surveys. These detection probabilities, which encompass all infections that occurred during the 1984–2013 period including asymptomatic infections, were distributed across several order of magnitude around 10^{-5}, but spatial heterogeneity was consistent between model variants (Table 1 and S2 Fig).

Both models consistently estimated the highest values of transmission intensity in terms of FOI and R_0 to be in West Africa and the lowest in Eastern Africa (Fig 2 and S3 Fig). Several provinces in Eastern and Central Africa had median R_0 estimates just above one—in reality these areas are likely not endemic for YF transmission, but the implicit assumption of endemic transmission in the R_0 model means it is unable to generate estimates of $R_0 < 1$. Local estimates of critical vaccination coverage (CVC), the threshold above which partial vaccination coverage is expected to protect the entire population, were derived from R_0 values (S4 Fig). For instance, in Côte d'Ivoire, CVC estimates ranged between 49% and 98% across provinces. Both model versions estimated vaccine efficacy at 0.95, with lower bound of the 95% credibility interval surrounding 0.70 (Table 1).

Results of the out-of-sample validation are presented in Fig 3 and S2 Appendix. Although uncertainty in the predictions were substantial, both model variants successfully reproduced heterogeneity in transmission intensity across provinces, particularly in South Sudan. Based on the likelihood criteria, out of nine study settings, the model variant providing the better predictions of the observed age-seroprevalence profiles was the FOI model in seven settings and the R0 model in two settings (S2 Appendix).

Estimates of the YF-specific burden are presented in Table 1 and Fig 4. We estimate 107,000 deaths (37,000–272,000) occurred in 2017 according to the FOI model and 30,000 (4,000–123,000) according to the R_0 model. As expected from its non-linear response to vaccination, the R_0 model was more sensitive to variations in vaccination coverage and predicted a
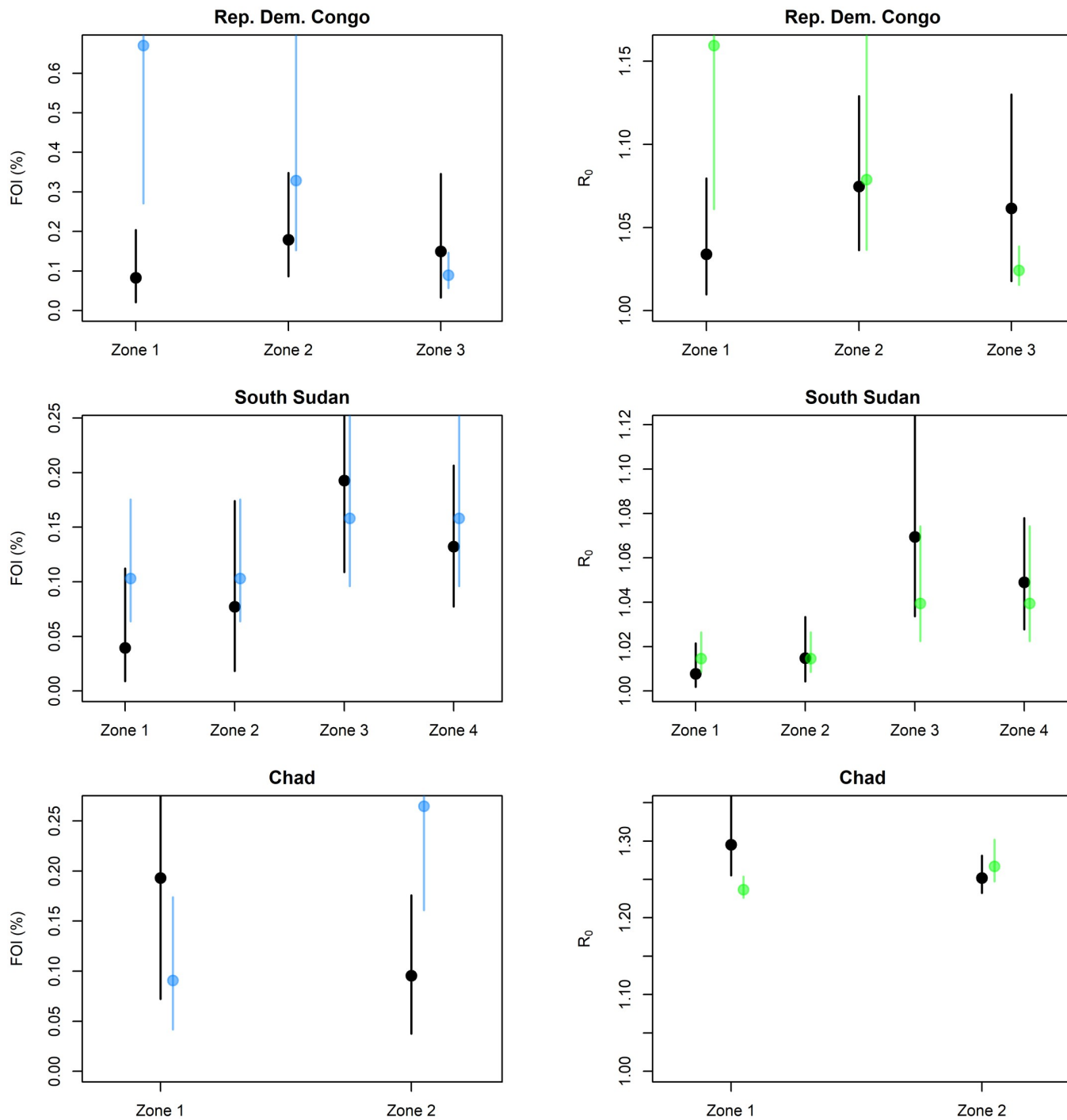
Fig 3. Comparison of directly estimated versus model-predicted transmission parameters for three external serological studies. Black: direct estimate; blue: prediction of the FOI model; green: prediction of the R_0 model. Lines show 95% credibility intervals.

higher burden than the FOI model before the implementation of mass vaccination campaigns (that is, before 2006), but a lower burden thereafter (S5 Fig). Of note, with no or low-level of vaccination coverage as in Eastern Africa, both model versions exhibited similar temporal trends (S6 Fig). Province-based burden estimates are presented in Fig 4. While the FOI model

Fig 4. Estimated 2017 incidence of severe yellow fever infection per 100,000 persons across 34 African countries. A: FOI model, B: R_0 model. For the R_0 model, provinces with no incidence are those for which the estimated vaccination coverage in 2017 was larger than the Critical Vaccination Coverage implied by R_0. Maps were produced from GADM version 2.0.
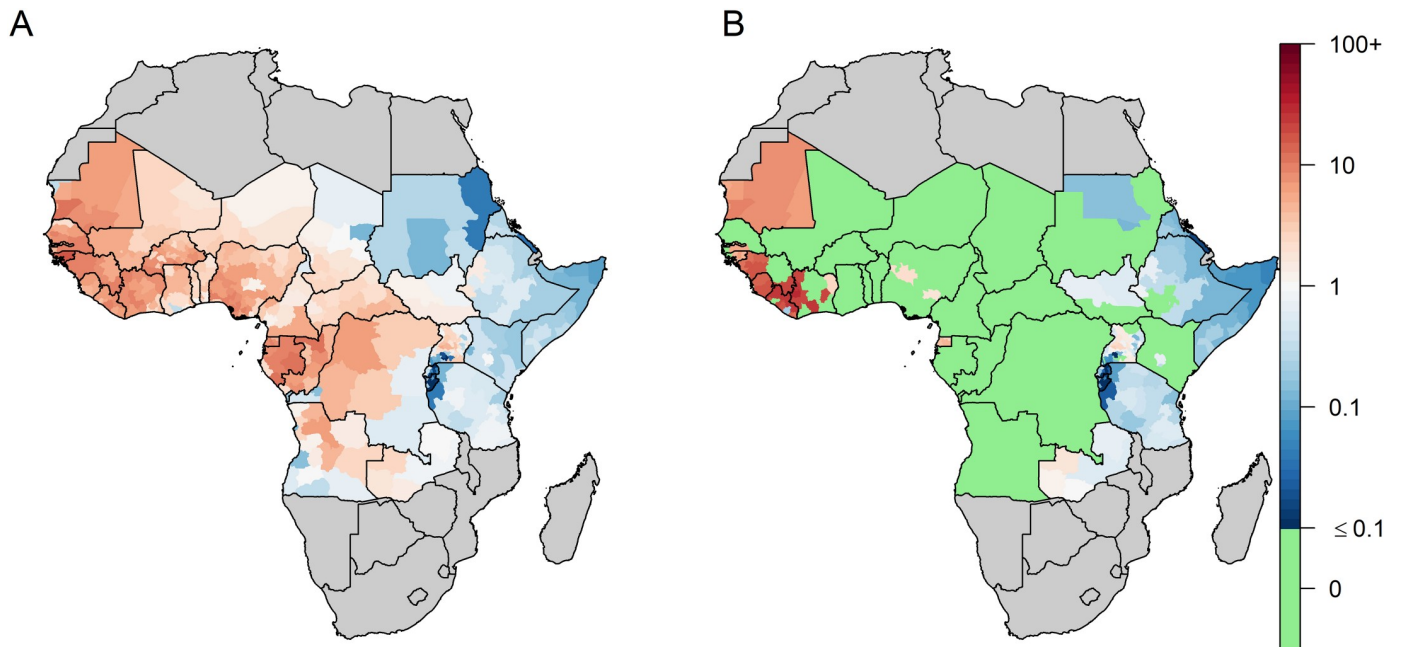
structure forced it to predict a non-zero force of infection, large parts of the endemic zone exhibited very low incidence rates (notably in Rwanda and Burundi). In contrast, the R_0 model predicted a zero incidence in all provinces where the vaccination coverage exceeded the local CVC. Large regions of Eastern Africa, that did not benefit from any vaccination activities, still exhibited small incidence rates in both model variants.

According to the FOI model, PMVCs conducted between 2005 and 2017 under the Yellow Fever Initiative [19] were estimated to have already prevented 700,000 (200,000–1,600,000) deaths as of 2017 and will prevent a further 2,600,000 (1,000,000–6,100,000) deaths over the lifetime of the vaccinees. According to the R_0 model, 2,600,000 (1,000,000–6,000,000) deaths have been prevented as of 2017 and 3,400,000 (1,300,000–7,400,000) future deaths will be prevented by those campaigns.

Fig 5 displays estimates of effective reproduction number R_{eff} in 2018, that is the transmission potential in a partially immune population, together with the categorisation (arbitrarily defined based on R_{eff}) of provinces for several PMVCs strategies. Due to low >1 R_0 values (by assumption) and non-existent vaccination coverage, large regions of Eastern Africa had estimates of $1.00 < R_{eff} < 1.01$. Assuming an optimal sequence for PMVC implementation (i.e. vaccinating first the provinces with the highest R_{eff} values), we estimated that an average annual number of 37.7 million doses would be sufficient to vaccinate all provinces with $R_{eff} \geq 1.01$ over the 2018–2026 period. Such a strategy would prevent 9,900,000 (7,000,000–13,400,000) infections and 480,000 (180,000–1,140,000) deaths over the lifetime of the vaccinees, corresponding to 1.7 (0.7–4.1) deaths averted per 1,000 vaccine doses (assuming no doses wasting) (Table 2). Broader strategies would result in larger number of deaths prevented at the cost of lower impact per doses.
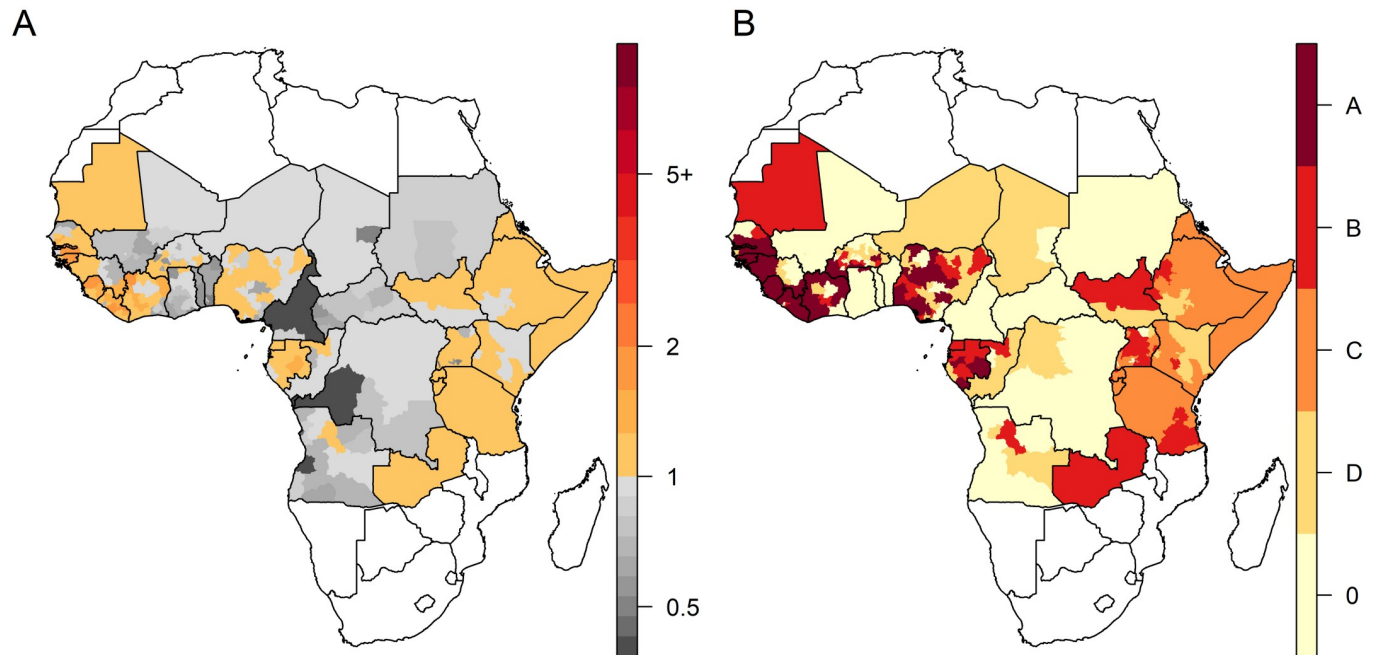
Fig 5. Estimates of the effective reproductive number (R_eff) and categorization for different preventive mass vaccination (PMVCs) strategies. A: estimates of the effective reproductive number (R_eff) based on 2018 vaccination coverage estimates; B: categorization for vaccination strategies. Each vaccination strategy includes all provinces from upper prioritization levels (ie the strategy B consists in vaccinating provinces corresponding to categories A and B). Light yellow provinces (R_eff<0.85) are not considered for PMVCs under any strategy. Maps were produced from GADM version 2.0.

https://doi.org/10.1371/journal.pntd.0008304.g005

Discussion

By combining a regression model fitted to the reported local presence of YF with serological data collected in 11 countries, this modelling study presents updated estimates of YF burden across 34 African countries in terms of number of infections, severe cases, deaths, and DALYs lost. We also estimated that PMVCs conducted since 2005 will prevent a total of 3 to 6 million deaths over the lifetime of vaccinees, depending on whether we disregard or maximize herd effects, respectively. As both sylvatic and urban transmission cycles (with none or maximal herd effects, respectively) do contribute to the disease burden, the real impact of vaccination

Table 2. Impact estimates of different preventive mass vaccination (PMVCs) strategies.

EYE strategy	Total target population (millions)	Average number of doses per year	Infections prevented	Deaths prevented	Deaths prevented per 1,000 vaccine doses*	% of deaths prevented
Strategy A (R_eff≥1.25)	143.9	18.0	1,378,000 (545,000–3,693,000)	66,000 (16,000–235,000)	0.5 (0.1–1.6)	3% (1–7%)
Strategy B (R_eff≥1.01)	277.9	37.7	9,888,000 (6,957,000–13,383,000)	481,000 (182,000–1,144,000)	1.7 (0.7–4.1)	19% (8–46%)
Strategy C Reff≥1.00	505.3	63.2	14,244,000 (10,317,000–19,746,000)	693,000 (270,000–1,607,000)	1.4 (0.5–3.2)	28% (11–73%)
Strategy D Reff≥0.85	644.4	83.1	15,141,000 (10,927,000–20,981,000)	736,000 (288,000–1,716,000)	1.1 (0.4–2.6)	29% (12–77%)

Infections and deaths prevented are calculated as the difference in the cumulative burden over the 2018–2100 time period between a scenario corresponding to the considered strategy and a baseline scenario assuming no future PMVCs. Infections include asymptomatic, mild and severe infections.

* assuming no doses wasting.

https://doi.org/10.1371/journal.pntd.0008304.t002

likely lies between these two extreme cases. Finally, we derived estimates of vaccine demand and impact of future PMVCs under a variety of targeted vaccination scenarios. We estimated that allocating a 37.7 million doses per year between 2018 and 2026 for PMVCs would prevent 9.89 (6.96–13.3) million YF infections and thus considerably reduce the risk of international spread.

The model we developed combines a risk-map derived from occurrence data with transmission intensity estimates in order to infer burden. Such an approach also provides valuable results for other diseases, such as dengue [20]. We estimated approximately 200,000 annual YF severe cases occurred before 2005 (S5 Fig), that is before the implementation of PMVCs in West Africa. These results are consistent with previous estimates suggested over the recent decades [13,21], while providing better insight about spatial and temporal heterogeneity in the burden of the disease, especially for the post-PMVCs period. Uncertainty in our results is substantial, covering more than one order of magnitude for some estimates. As our model integrates all existing data on YF that are currently available for Africa, such uncertainty reflects the current lack of accurate knowledge regarding YF incidence and epidemiology.

The two model variants we developed exhibited substantial differences in resulting estimates of YF burden and vaccine impact, especially for the recent period. By integrating herd effects as an important component of urban transmission, the impact of vaccination estimated in the R_0 model was roughly twice that estimated in the FOI model, which represents sylvatic transmission. Cases' characteristics and environmental assessment suggested a sylvatic origin of the 2016 Uganda outbreak [22]. Similarly, the lack of a large number of urban cases indicates a primarily sylvatic source for the 2017–2018 Nigeria outbreak [2]. On the contrary, the 2016 YF outbreak in Angola provided evidence of a large contribution of the urban transmission cycle [23]. None of these model variants we developed was correct, as both were considering a unique YF transmission cycle, and neither model performed systematically better than the other in predicting transmission intensity, suggesting that the transmission cycle to preferably consider may depend on the setting. The estimates from both models should therefor by seen as two extreme scenarios of sylvatic or human-to-human, transmission only, with no or maximized herd effects, respectively. The reality of yellow fever transmission probably lies within these bounds. Better understanding the relative contribution of the different transmission routes may affect control strategies. While vaccination prevents both sylvatic and urban transmission, vector population control interventions appear relevant in urban settings but may not be feasible to protect populations exposed to sylvatic mosquitoes. A recent study tried to disentangle the contribution of each transmission cycle in Brazil [12]. However, this analysis relied on detailed spatiotemporal and genomic data not currently available for Africa.

Assumptions on the global contribution of both transmission cycles have important effects on vaccine impact estimates, which in turn may impact prioritization across diseases by vaccine funders. By disregarding herd immunity, the FOI model version likely produces underestimates of vaccine impact. This model variant may thus be preferred for a conservative estimates of vaccine impact and demand. However, the R_0 model version remains of interest to produce "best-case" scenario of vaccine impact maximizing herd effects. Moreover, the R_0 model can be used to derive important epidemiological parameters, such as the CVC, for specific contexts where zoonotic transmission is unlikely (mostly, urban contexts). Combining estimates of model variants that rely on different assumptions and structures in a way that can reliably inform decision making remains a challenge. Bayesian model averaging methods have been suggested to better combine such estimates [24].

The models used to estimate the burden and subsequently the impact of vaccination are fitted to data of reported YF events over a 30-years period in order to smooth over the long and irregular cycles of epidemic activity sweeping across the continent, such as the re-emergence

during 1985–95 [25]. These data show a pattern of near-ubiquitous presence in large swathes of West Africa, with more patchy presence in Central and East Africa, which in turn determine the gradient in transmission intensity seen in the model. Due to the very widespread YF presence in West Africa, the model lacks resolution for estimating the exact level of transmission intensity in this area. Under-reporting of cases and transmission intensity are estimated by fitting serological surveys data from Central and Eastern Africa. Unfortunately, high quality surveys from West Africa are lacking. Of note, our validation assessment revealed that the model produces reasonable predictions across settings exhibiting varying levels of seroprevalence (S2 Appendix). This may be seen as a case for the validity of our model across a range of transmission intensity levels.

Our estimates of under-reporting of the disease (ranging between 10^{-7} and 10^{-5}) may appear low at first glance. However, there are several considerations to keep in mind when interpreting these estimates. Firstly, these are estimates of per-infection detection probability, while only about 10% of all infections are estimated to lead to severe disease [18]. Secondly, the symptoms associated with mild or even severe yellow fever infections are wide and non-specific. This leads to cases being frequently confused with severe malaria, leptospirosis, viral hepatitis or infections with other flaviviruses. Thirdly, our under-reporting estimates constitute an average over a 30-year time period (1984–2013). Regional capacities for laboratory confirmation of diagnostic was quite limited over a large part of this time period [21]. During this time period, official case detection reported the virtual absence of reported cases in some years [13], while the annual burden was estimated around 200,000 cases at the same time [21].

While the FOI model variant assumes a constant local infection risk for those unvaccinated, the R_0 model variant relies on the assumption of endemic equilibrium, which allows long periods without transmission if population-level vaccination coverage exceeds the CVC and therefore suppresses transmission [26]. While for an epidemic disease this might appear an unrealistic assumption, one can consider that over the course of many years the higher incidence during epidemics balances the low incidence in inter-epidemic periods to achieve the equilibrium level on average. The endemic equilibrium assumption might also appear unrealistic for low transmission settings, especially in Eastern Africa. However, both model variants were designed in order to converge in the absence of vaccination. Thus, in large regions of Eastern Africa with no history of vaccination, both model variants resulted in similar burden estimates (S6D Fig). We can thus consider that the endemic equilibrium assumption did not yield to massive overestimation in the disease burden for low-transmission settings. Neither model variant completely captures the epidemic character of the disease driven by rapid depletion of susceptible hosts during explosive outbreaks, slow host renewal in inter-epidemic periods and sporadic disease reintroductions. By design, these models are also unable to account for short-term changes in disease transmission that could have resulted from recent changes in land use or other ecosystems degradation. Instead, these models were designed to capture spatial heterogeneity in the burden and estimate long-term average vaccine impact.

Both model fitting and projections are based on vaccine-coverage estimates derived from a demographic model combining different sources of data regarding vaccination activities [15]. A majority of the data related to past vaccination activities are available under the form of the coverage achieved in specific areas. Transforming achieved coverage back into a number of doses would require numerous assumptions in term of doses wasting or multiple doses for the same individual. Estimating the number of vaccine doses for past activities could thus lead to overestimation of past vaccination effectiveness that would be difficult to quantify. Concurrent estimates for vaccine coverage have been recently developed [27]. Although overall consistent with ours, these estimates appeared to disregard several recent large-scale campaigns in West and Central Africa [15]. Uncertainty in vaccination coverage is not directly accounted for in

our model, but may be propagated in the vaccine efficacy parameter. Indeed, the posterior distribution of vaccine efficacy is much wider than the range documented in a recent meta-analysis [16], especially for the R_0 variant which is expected to be more sensitive to vaccine coverage. Lastly, in the absence of more detailed data, vaccination activities were often assumed to be implemented homogeneously across space in particular for routine immunization, glossing over existing heterogeneities in coverage. Recent efforts to document such heterogeneity, such as the YF EPI warning system developed by the WHO, are thus welcome [28].

Our model has several limitations but also some strengths compared with past work. We captured spatial heterogeneity in the disease using a statistical rather than a mechanistic approach. Our model does not explicitly represent the spatial distribution of vectors nor disease reservoirs unlike Shearer et al's model [10]. However, the set of spatial predictors we used has been demonstrated to have good predictive power for both presence and seasonality of YF [29]. Moreover, the environmental covariate we used as spatial predictor for case reports are frequently used to predict the spatial distribution of vectors or reservoirs [30,31]. To our knowledge, our model is the only one calibrated against serological data that captures the whole spectrum of disease severity. Other YF burden estimates stem from models calibrated on reported cases [10,32], that may lead to underestimation due to under-reporting and misdiagnosis. For instance, the Global Burden of Disease estimates for 2016 around 5,000 YF-deaths in Africa, which is near to the lower bound of our R_0 model estimates. Lastly, the development of the R_0 variant of our model constitutes a novel approach to account for herd effects in the impact of YF vaccination. Our results highlight that heterogeneity in transmission intensity imply different vaccination threshold to be reached in order to prevent YF outbreaks. This can be used to locally adapt the empirical threshold of 80% vaccination coverage that is often considered sufficient for YF outbreak prevention [11].

Using local estimates of the potential for urban outbreaks for PMVCs prioritization, we explored several vaccination scenarios ranking from a parsimonious strategy focussed on high-risk areas to an ambitious large-scale approach targeting the vast majority of provinces within the at-risk region. The individual assessment for each strategy was conducted under optimistic assumptions, thus resulting expected vaccine impact is overestimated; however this choice may not have massively affected the comparison across strategies. Recent years have shown that efforts to control YF outbreaks were highly constrained by the stock of vaccine doses available for emergency situation [33]. Optimal vaccine allocation is also crucial in the context of preventive vaccination activities. By contrasting the impact of several scenarios with the corresponding vaccine demand, and also by suggesting a sequence of implementation within each scenario, this study helps in the search for optimal vaccine allocation. We do acknowledge however that a realistic strategy will need to take into account further factors such as operational or political concerns.

Patterns of YF transmission seem to have changed in the recent years toward shorter transition from the sylvatic cycle to urban inter-human transmission [5]. Renewed disease control strategies thus need to account for this change in implementation of control measures. This study addressed this challenge by developing a vaccine impact modelling framework accounting for urban YF transmission. This work has contributed to a risk assessment conducted as part of the EYE strategy in order to prioritize countries for PMVCs [34].

Supporting information

S1 Table. Presence or absence of any reported yellow fever event between 1984 and 2013 at the first sub-national administrative level in 34 African countries.
(CSV)

S1 Appendix. Model description.
(DOCX)

S2 Appendix. Model validation.
(DOCX)

S1 Fig. Observed versus predicted presence/absence of any yellow fever reported event between 1984 and 2013. A: Presence (red) or absence (white) of YF report between 1984 and 2013, B: GLM prediction for probability of report for the FOI model; C: GLM prediction for probability of report for the R0 model. GLM: Generalized Linear Model. Maps were produced from GADM version 2.0.
(DOCX)

S2 Fig. Country-specific per-infection probability of detection across both model variants. A: FOI model, B: R_0 model. Maps were produced from GADM version 2.0.
(DOCX)

S3 Fig. Variability in the estimates of transmission intensity across model variants. A: coefficient of variation of the force of infection estimates; B: coefficient of variation of the R_0 estimates. Maps were produced from GADM version 2.0.
(DOCX)

S4 Fig. Estimated median critical vaccination coverage (A, %) and interquartile range in the critical vaccination coverage (B, %). R0 model. Maps were produced from GADM version 2.0.
(DOCX)

S5 Fig. Comparison of yellow fever burden estimates over time between both model versions across the whole endemic region (34 countries). Light blue lines: individual FOI model runs, 1,000 simulations. Dark blue line: median FOI model burden. Blue region: 95% Credible Interval of the FOI model burden. Light green lines: individual R0 model runs, 1,000 simulations. Dark green line: median R0 model burden. Green region: 95% Credible Interval of the FOI model burden. Grey line: overall population-level vaccination coverage across the whole endemic region.
(DOCX)

S6 Fig. Comparison of yellow fever burden estimates over time between both model versions across sub-regions. Light blue lines: individual FOI model runs, 1,000 simulations. Dark blue line: median FOI model burden. Blue region: 95% Credible Interval of the FOI model burden. Light green lines: individual R0 model runs, 1,000 simulations. Dark green line: median R0 model burden. Green region: 95% Credible Interval of the FOI model burden. Grey line: overall population-level vaccination coverage across the sub-region. A: Sahel region; B: western Africa; C: central Africa; D: eastern Africa; E: sub-regions definition. Maps were produced from GADM version 2.0.
(DOCX)

Acknowledgments

Author Contributions

Conceptualization: Neil M. Ferguson, Tini Garske.

Data curation: Kévin Jean, Arran Hamlet, Tini Garske.

Formal analysis: Kévin Jean, Arran Hamlet, Tini Garske.

Funding acquisition: Neil M. Ferguson, Tini Garske.

Investigation: Amadou Sall, Tini Garske.

Methodology: Kévin Jean, Neil M. Ferguson, Tini Garske.

Project administration: Neil M. Ferguson, Tini Garske.

Resources: Justus Benzler, Laurence Cibrelus, Amadou Sall, Neil M. Ferguson, Tini Garske.

Software: Kévin Jean, Arran Hamlet, Katy A. M. Gaythorpe, Tini Garske.

Supervision: Neil M. Ferguson, Tini Garske.

Validation: Kévin Jean.

Visualization: Kévin Jean, Tini Garske.

Writing – original draft: Kévin Jean.

Writing – review & editing: Kévin Jean, Arran Hamlet, Justus Benzler, Laurence Cibrelus, Katy A. M. Gaythorpe, Amadou Sall, Neil M. Ferguson, Tini Garske.

References

1. WHO. Yellow fever in Africa and the Americas, 2016. Wkly Epidemiol Rec WER. 2017; 92: 442–452. PMID: 28799735

2. Disease Outbreak News. Yellow fever—Nigeria. Dis Outbreak News—WHO. 2017 [cited 9 Jan 2018]. http://www.who.int/csr/don/22-december-2017-yellow-fever-nigeria/en/

3. Wang L, Zhou P, Fu X, Zheng Y, Huang S, Fang B, et al. Yellow fever virus: Increasing imported cases in China. J Infect. 2016; 73: 377–380. https://doi.org/10.1016/j.jinf.2016.07.003 PMID: 27422700

4. Nishino K, Yactayo S, Garcia E, Aramburu G, Manuel E, Costa A, et al. Yellow fever urban outbreak in Angola and the risk of extension. Wkly Epidemiol Rec WER. 2016; 91: 181–192.

5. World Health Organization. Eliminate Yellow fever Epidemics (EYE): a global strategy, 2017–2026. Wkly Epidemiol Rec. 2017; 92: 193–204. PMID: 28429585

6. Kraemer MUG, Faria NR, Reiner RC, Golding N, Nikolay B, Stasse S, et al. Spread of yellow fever virus outbreak in Angola and the Democratic Republic of the Congo 2015–16: a modelling study. Lancet Infect Dis. 2016. https://doi.org/10.1016/S1473-3099(16)30513-8 PMID: 28017559

7. Zhao S, Stone L, Gao D, He D. Modelling the large-scale yellow fever outbreak in Luanda, Angola, and the impact of vaccination. PLoS Negl Trop Dis. 2018; 12: e0006158. https://doi.org/10.1371/journal.pntd.0006158 PMID: 29338001

8. Rogers DJ, Wilson AJ, Hay SI, Graham AJ. The global distribution of yellow fever and dengue. Adv Parasitol. 2006; 62: 181–220. https://doi.org/10.1016/S0065-308X(05)62006-4 PMID: 16647971

9. Garske T, Van Kerkhove MD, Yactayo S, Ronveaux O, Lewis RF, Staples JE, et al. Yellow Fever in Africa: Estimating the Burden of Disease and Impact of Mass Vaccination from Outbreak and Serological Data. PLoS Med. 2014; 11: e1001638. https://doi.org/10.1371/journal.pmed.1001638 PMID: 24800812

10. Shearer FM, Longbottom J, Browne AJ, Pigott DM, Brady OJ, Kraemer MUG, et al. Existing and potential infection risk zones of yellow fever worldwide: a modelling analysis. Lancet Glob Health. 2018; 0. https://doi.org/10.1016/S2214-109X(18)30024-X PMID: 29398634

11. World Health Organization. Yellow fever key facts. 1 May 2018. http://www.who.int/en/news-room/fact-sheets/detail/yellow-fever

12. Faria NR, Kraemer MUG, Hill SC, de Jesus JG, Aguiar RS, Iani FCM, et al. Genomic and epidemiological monitoring of yellow fever virus transmission potential. Science. 2018; eaat7115. https://doi.org/10.1126/science.aat7115 PMID: 30139911

13. Monath TP, Vasconcelos PFC. Yellow fever. J Clin Virol. 2015; 64: 160–173. https://doi.org/10.1016/j.jcv.2014.08.030 PMID: 25453327

14. Anderson R, May RM. Infectious Diseases of Humans: Dynamics and Control. 2nd edn. Oxford University Press; 1991.

15. Hamlet A, Jean K, Yactayo S, Benzler J, Cibrelus L, Ferguson N, et al. POLICI: A web application for visualising and extracting yellow fever vaccination coverage in Africa. Vaccine. 2019; 37: 1384–1388. https://doi.org/10.1016/j.vaccine.2019.01.074 PMID: 30770224

16. Jean K, Donnelly CA, Ferguson NM, Garske T. A Meta-Analysis of Serological Response Associated with Yellow Fever Vaccination. Am J Trop Med Hyg. 2016; 95: 1435–1439. https://doi.org/10.4269/ajtmh.16-0401 PMID: 27928091

17. Gotuzzo E, Yactayo S, Córdova E. Efficacy and duration of immunity after yellow fever vaccination: systematic review on the need for a booster every 10 years. Am J Trop Med Hyg. 2013; 89: 434–444. https://doi.org/10.4269/ajtmh.13-0264 PMID: 24006295

18. Johansson MA, Vasconcelos PFC, Staples JE. The whole iceberg: estimating the incidence of yellow fever virus infection from the number of severe cases. Trans R Soc Trop Med Hyg. 2014; 108: 482–487. https://doi.org/10.1093/trstmh/tru092 PMID: 24980556

19. WHO, UNICEF. Yellow Fever Initiative Joint WHO and UNICEF 2010 Progress Report. Geneva, Switzerland: World Health Organisation; 2010.

20. Bhatt S, Gething PW, Brady OJ, Messina JP, Farlow AW, Moyes CL, et al. The global distribution and burden of dengue. Nature. 2013; 496: 504–507. https://doi.org/10.1038/nature12060 PMID: 23563266

21. World Health Organization. Yellow fever vaccine. Wkly Epidemiol Rec. 2003; 349–359.

22. Kwagonza L, Masiira B, Kyobe-Bosa H, Kadobera D, Atuheire EB, Lubwama B, et al. Outbreak of yellow fever in central and southwestern Uganda, February-may 2016. BMC Infect Dis. 2018; 18: 548. https://doi.org/10.1186/s12879-018-3440-y PMID: 30390621

23. Bagcchi S. Looking back at yellow fever in Angola. Lancet Infect Dis. 2017; 17: 269–270. https://doi.org/10.1016/S1473-3099(17)30064-6 PMID: 28244394

24. Gaythorpe KAM, Jean K, Cibrelus L, Garske T. Quantifying model evidence for yellow fever transmission routes in Africa. PLOS Comput Biol. 2019; 15: e1007355. https://doi.org/10.1371/journal.pcbi.1007355 PMID: 31545790

25. Robertson SE, Hull BP, Tomori O, Bele O, LeDuc JW, Esteves K. Yellow fever: a decade of reemergence. JAMA. 1996; 276: 1157–1162. PMID: 8827969

26. Fine P, Eames K, Heymann DL. "Herd immunity": a rough guide. Clin Infect Dis Off Publ Infect Dis Soc Am. 2011; 52: 911–916. https://doi.org/10.1093/cid/cir007 PMID: 21427399

27. Shearer FM, Moyes CL, Pigott DM, Brady OJ, Marinho F, Deshpande A, et al. Global yellow fever vaccination coverage from 1970 to 2016: an adjusted retrospective analysis. Lancet Infect Dis. 2017; 0. https://doi.org/10.1016/S1473-3099(17)30419-X PMID: 28822780

28. World Health Organization. Yellow fever in Africa and South America, 2015. Wkly Epidemiol Rec. 2016; 91: 381–388. PMID: 27522678

29. Hamlet A, Jean K, Perea W, Yactayo S, Biey J, Kerkhove MV, et al. The seasonal influence of climate and environment on yellow fever transmission across Africa. PLoS Negl Trop Dis. 2018; 12: e0006284. https://doi.org/10.1371/journal.pntd.0006284 PMID: 29543798

30. Kraemer MUG, Sinka ME, Duda KA, Mylne AQN, Shearer FM, Barker CM, et al. The global distribution of the arbovirus vectors Aedes aegypti and Ae. albopictus. eLife. 2015; 4: e08347. https://doi.org/10.7554/eLife.08347 PMID: 26126267

31. de Almeida MAB, dos Santos E, Cardoso J da C, da Silva LG, Rabelo RM, Bicca-Marques JC. Predicting Yellow Fever Through Species Distribution Modeling of Virus, Vector, and Monkeys. EcoHealth. 2018 [cited 7 Jan 2019]. https://doi.org/10.1007/s10393-018-1388-4 PMID: 30560394

32. Vos T, Allen C, Arora M, Barber RM, Bhutta ZA, Brown A, et al. Global, regional, and national incidence, prevalence, and years lived with disability for 310 diseases and injuries, 1990–2015: a systematic analysis for the Global Burden of Disease Study 2015. The Lancet. 2016; 388: 1545–1602. https://doi.org/10.1016/S0140-6736(16)31678-6 PMID: 27733282

33. Monath TP, Woodall JP, Gubler DJ, Yuill TM, Mackenzie JS, Martins RM, et al. Yellow fever vaccine supply: a possible solution. The Lancet. 2016; 387: 1599–1600. https://doi.org/10.1016/S0140-6736(16)30195-7

34. Global Strategy to Eliminate Yellow fever Epidemics (EYE)—Document for SAGE. World Health Organisation; 2016 Sep. http://www.who.int/immunization/sage/meetings/2016/october/2_EYE_Strategy.pdf